A local normal-based region term for active contours

Julien MILLE and Laurent D. COHEN

CEREMADE, CNRS UMR 7534, Université Paris Dauphine
Place du Maréchal de Lattre de Tassigny, 75775 Paris, France
{mille,cohen}@ceremade.dauphine.fr

Abstract. Global region-based active contours, like the Chan-Vese model, often make strong assumptions on the intensity distributions of the searched object and background, preventing their use in natural images. We introduce a more flexible local region energy achieving a trade-off between local features of gradient-like terms and global region features [1]. Relying on the theory of parallel curves, we define our region term using constant length lines normal to the contour. Mathematical derivations are performed on an explicit curve, leading to a form allowing efficient implementation on a parametric snake. However, we provide implementations on both explicit and implicit contours.

1 Introduction

Active contours, whether parametric [1] or level-set based [2], were initially attached to data by means of edge-based terms. The increasing use of region terms inspired by the Mumford-Shah functional [3][4] has proven to overcome limitations of gradient-based only models, especially when dealing with data sets suffering from noise and lack of contrast between neighboring structures. Early work including the mixed model of Cohen *et al* [5] and the active region model by Ivins and Porrill [6] introduced the use of region terms in the evolution of parametric snakes. On the other hand, many papers have dealt with region-based approaches using the level set framework, including the active contours without edges by Chan and Vese [7], the deformable regions by Jehan-Besson *et al* [8] and the geodesic active regions by Paragios and Deriche [9], benefiting of adaptive topology at the expense of computational cost. Classical region-based deformable models segment images according to statistical data computed over the object of interest and the background. Image partitions should be uniform in terms of pixel intensities or higher level features like texture descriptors [9]. Considering for instance the Chan-Vese model [7], the region term penalizes the curve splitting the image into heterogeneous regions, using intensity variances. It is devoted by essence to the segmentation of uniform objects and backgrounds.

[1] This work was partially supported by ANR grant MESANGE ANR-08-BLAN-0198

Such an ideal case is rarely encountered in most of computer vision applications, as the background usually contains various structures, which differ in their overall intensities or textures. In this context, the multiphase approach [10] allows to partition the image into more than two regions, provided that the number of partitions is known. When one wishes to extract a particular object from the background without any prior knowledge about the number of actual regions, strict homogeneity is not desirable property for the background. In order to account for spatially varying intensity, local statistics in region-based segmentation have emerged recently [11][12][13][14]. Basically, these methods express the data term as a sum of local region energies computed over neighborhoods of pixels inside and outside the evolving curve. We believe these approaches have the drawback of not formulating the region energy fully explicitly in terms of the curve, which only leads to a level set implementation. However, many applications benefit from explicit implementations of active contours, including low computational cost and topological control. This justifies the use of an explicit mathematical framework.

We introduce a local normal-based region energy handling configurations in which the outer neighborhood of the object is piecewise uniform. Unlike other region terms, whether local or global, this new type of combination allows to handle the common case where one seeks for a uniform object in a heterogeneous background. We formulate it as the intensity variance over the inner region and finite length lines along outward normals to the curve. The theory of parallel curves [15][16] leads to an explicit formulation of our energy, which is suitable for mathematical derivation and implementation on parametric contours. In order to allow gradient descent afterwards, we determine the variational derivative of the region energy thanks to calculus of variations. Then, we deal with numerical implementation on both parametric snakes and level sets. Finally, experiments are carried out on medical data and natural color images. The tests present the advantages of our new data term over an edge term, a global region term as well as a recent local region-based approach [12].

2 Local normal-based region energy

2.1 Active contour model

Given a simple closed curve Γ with position vector $\mathbf{c}(u) = [x(u)\ y(u)]^T$ with $u \in \Omega = [0, 1]$, segmentation is performed by finding the curve minimizing a weighted sum of smoothness term and our local normal-based region (LNBR) energy:

$$E[\Gamma] = \omega E_{\text{smooth}}[\Gamma] + (1 - \omega) E_{\text{LNBR}}[\Gamma] \tag{1}$$

where the user-provided ω weights the significance of the smoothness term, which can be classicaly written with squared magnitudes of first and second order derivatives. Curve Γ splits the image domain $\mathcal{D}$ into an inner region R_{I} and an outer region R_{O}. Instead of formulating our data term on R_{I} and R_{O}, we

use the narrow band principle, which has proven its efficiency in the evolution of level sets [2]. Hence, in addition to the inner region R_{I}, instead of dealing with the entire image domain, we consider an outer band $\mathcal{B}_{\mathrm{O}}$ in the vicinity of Γ, as depicted in fig. 1.

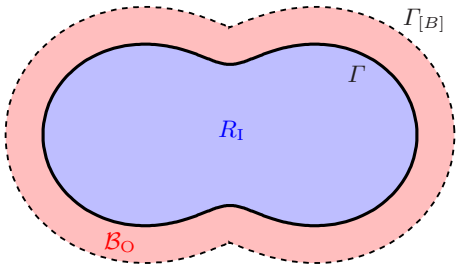

Fig. 1. Inner region and outer band for LNBR energy

The purpose of the LNBR energy is to handle cases where the inner region is homogeneous and the background is locally homogeneous in the outer band. For now, we express the outer term using a local descriptor depending on current position $\mathbf{x}$:

$$E_{\mathrm{LNBR}}[\Gamma] = \iint_{R_{\mathrm{I}}} (I(\mathbf{x}) - \mu_{\mathrm{I}})^2 d\mathbf{x} + \iint_{\mathcal{B}_{\mathrm{O}}} (I(\mathbf{x}) - \mu(\mathcal{B}_{\mathrm{O}}, \mathbf{x}))^2 d\mathbf{x} \tag{2}$$

In what follows, we explain how E_{LNBR} can be explicitly formulated in terms of curve Γ.

2.2 Parallel curve

Let B be the band thickness, constant along Γ. The theoretical background of our narrow band framework is based on parallel curves [15][16]. The curve $\Gamma_{[B]}$ is called a parallel curve of Γ, as its position vector $\mathbf{c}_{[B]}$ is defined by:

$$\mathbf{c}_{[B]}(u) = \mathbf{c}(u) - B\mathbf{n}(u) \tag{3}$$

where $\mathbf{n}$ is the unit inward normal. Hereafter, we will use the index $[B]$ to denote all quantities related to the parallel curve. The definition in eq. (3) is suitable to our narrow band formulation, in the sense that $\mathcal{B}_{\mathrm{O}}$ is bounded by Γ and $\Gamma_{[B]}$. Afterwards, we denote $R_{\mathrm{I}[B]}$ the dilated inner region bounded by $\Gamma_{[B]}$.

Given length element $\|\mathbf{c}_u\|$ and curvature κ, an important property resulting from the definition in eq. (3) is that the velocity vector of the parallel curve can

be expressed as a function of the velocity vector of Γ, as well as its curvature and normal. Using the identity $\mathbf{n}_u = -\kappa \mathbf{c}_u$, we have:

$$\mathbf{c}_{[B]_u} = \mathbf{c}_u - B\mathbf{n}_u = (1 + B\kappa)\mathbf{c}_u \tag{4}$$

and the corresponding length element is $\left\|\mathbf{c}_{[B]_u}\right\| = |1+B\kappa| \, \|\mathbf{c}_u\|$, which implies a constraint on the maximal curvature of curve Γ. We should assume that Γ is smooth enough so that $\kappa(u) > -1/B$, $\forall u \in \Omega$, so that curve $\Gamma_{[B]}$ does not exhibit singularities. This has an impact on explicit numerical implementation, which is discussed in section 3.1.

We rely on the principle of parallel curve to transform region integrals over $\mathcal{B}_{\mathrm{O}}$. Introducing a variable thickness b and using Green's theorem to convert region integrals into boundary integrals, it can be shown that:

$$\iint_{\mathcal{B}_{\mathrm{O}}} f(\mathbf{x}) d\mathbf{x} = \int_{\Omega} \int_{0}^{B} f(\mathbf{c} - b\mathbf{n}) \, \|\mathbf{c}_u\| \, (1 + b\kappa) db du \tag{5}$$

2.3 Transformation and derivation of LNBR energy

We provide the final expression of the LNBR term as it is implemented, in contrast with the temporary form of eq. (2). We now assume that piecewise uniformity over the outer band is verified if intensity is uniform along line segments in the direction normal to the object boundary. We first calculate the average intensity along the outward local normal line of length B at a given contour point. We use the same curvature-dependent weighting than in eq. (5), leading to:

$$\mu_{\mathrm{LN}}(u) = \frac{2}{B(2 + B\kappa)} \int_{0}^{B} I(\mathbf{c} - b\mathbf{n})(1 + b\kappa) db \tag{6}$$

where $I(\mathbf{x}) \in [0, 1]$ is the image intensity. The LNBR energy should penalize non-uniformity over the whole inner region and over all normal lines. Thus, we write:

$$E_{\mathrm{LNBR}}[\Gamma] = \iint_{R_{\mathrm{I}}} (I(\mathbf{x}) - \mu_{\mathrm{I}})^2 d\mathbf{x} + \int_{\Omega} \|\mathbf{c}_u\| \int_{0}^{B} (I(\mathbf{c} - b\mathbf{n}) - \mu_{\mathrm{LN}}(u))^2 (1 + b\kappa) db du \tag{7}$$

where μ_{I} is the average intensity of inner region R_{I}. To some extent, the outer band $\mathcal{B}_{\mathrm{O}}$ is split into infinitesimal trapezoids with parallel sides $\|\mathbf{c}_u\|$ and $\|\mathbf{c}_u\| \, (1+B\kappa)$. This principle is represented on the discretized curve in fig. 2. The LNBR energy has the following first variation (details of derivation are provided in the appendix):

$$\frac{\delta E_{\mathrm{LNBR}}}{\delta \Gamma} \approx \|\mathbf{c}_u\| \left[-(I(\mathbf{c}) - \mu_{\mathrm{I}})^2 - (1 + B\kappa)(I(\mathbf{c}_{[B]}) - \mu_{\mathrm{LN}})^2 + (I(\mathbf{c}) - \mu_{\mathrm{LN}})^2 \right] \mathbf{n} \tag{8}$$

The derivative holds the term $(I(\mathbf{c})-\mu_{\mathrm{LN}})^2 - (I(\mathbf{c})-\mu_{\mathrm{I}})^2$, which is clearly in accordance with the region-based segmentation principle. Indeed, the sign of the above quantity depends on the likeness of the current point's intensity with respect to μ_{I} or μ_{LN}. If $I(\mathbf{c})$ is closer to μ_{I} than μ_{LN}, the contour will locally expand, as it would be the case with a region growing approach. The derivative holds an additional curvature-dependent term which effect is discussed in section 3.1.

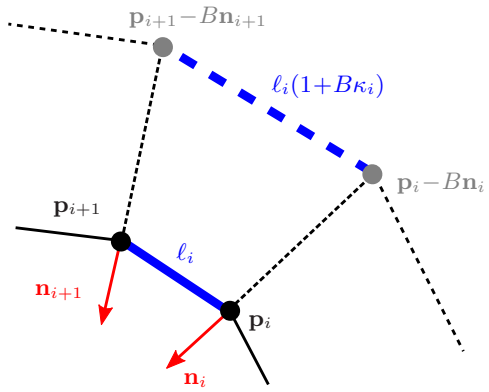

Fig. 2. Neighboring vertices with corresponding points on the discrete parallel curve

3 Numerical implementation

3.1 Explicit representation

Implementation on an explicit curve is pertinent when speed and topology preservation is a major concern. The contour is discretized as a closed polygonal line made up of a set of n vertices, denoted $\mathbf{p}_i = [x_i \; y_i]^T$. Their coordinates are iteratively modified using gradient descent of eq. (1):

$$\mathbf{p}_i^{(t+1)} = \mathbf{p}_i^{(t)} + \Delta t \mathbf{f}(\mathbf{p}_i) \tag{9}$$

where $\mathbf{f}(\mathbf{p}_i)$ is the force vector depending on the discretization of the energy derivative at a given vertex $\mathbf{p}_i$. In addition to the squared differences between $I(\mathbf{c})$ and the average intensities, the variational derivative in eq. (8) also contains a curvature-based term depending on the intensity at point $\mathbf{c}_{[B]}$. Actually, this term turns out to go against the region growing or shrinking principle, as it opposes the other terms depending on $I(\mathbf{c})$. As stated in [17], the usual energy gradient may not be systematically the best direction to take, which justifies our choice to remove side effect terms. The region force is:

$$\mathbf{f}_{\mathrm{LNBR}}(\mathbf{p}_i) = \left[(I(\mathbf{p}_i)-\mu_{\mathrm{I}})^2 - (I(\mathbf{p}_i)-\mu_{\mathrm{LN}}(\mathbf{p}_i))^2\right] \mathbf{n}_i \tag{10}$$

Given ℓ_i, $\mathbf{n}_i$ and κ_i the finite differences discretizations of length element, normal and curvature at vertex $\mathbf{p}_i$, the average intensity along the normal line is implemented as:

$$\mu_{\mathrm{LN}}(\mathbf{p}_i) = B\left(1 + \frac{\kappa_i(B+1)}{2}\right)\sum_{b=1}^{b=B}(1+b\kappa_i)I(\mathbf{p}_i - b\mathbf{n}_i)$$

Fig. 2 depicts two neighboring vertices on a locally convex polygon, with corresponding length elements and points on the parallel polygon. There are two complementary techniques to address the regularity condition $\kappa_i > -1/B$. The first one is to prevent vertices from making sharp angles with their neighbors, so that κ_i is well bounded. Moreover, the case of a negative length element can be handled. Hence, $\ell_i(1+b\kappa_i)$ is actually computed as $\max(0, \ell_i(1+b\kappa_i))$.

In a particular case, the formulation of $\mathbf{f}_{\mathrm{LNBR}}$ presents a shortcoming. Indeed, the magnitude of $\mathbf{f}_{\mathrm{LNBR}}$ is low when μ_{I} and μ_{LN} are similar. This situation also arises in local region-based methods [12][13] when the curve, including the outer neighborhood, is initialized inside a uniform area. However, we expect the contour to grow if the intensity at the current vertex matches the inner region features, whatever the value of μ_{LN}. Thus, we introduce a bias acting like a balloon force [18] which expands the boundary in the normal direction:

$$\mathbf{f}_{\mathrm{bias}}(\mathbf{p}_i) = -\alpha(1 - (\mu_{\mathrm{I}} - \mu_{\mathrm{LN}}(\mathbf{p}_i))^2)\mathbf{n}_i \tag{11}$$

with $\alpha \in [0, 1]$. Forces $\mathbf{f}_{\mathrm{LNBR}}$ and $\mathbf{f}_{\mathrm{bias}}$ are summed up, so that the bias is predominant when mean intensities are close. Consequently, we do not loose the convergence ability of global region-based active contours. The region bias guarantees the contour has a similar capture range as global region-based contours.

Let us give a note on the implementation of Green's theorem. Our experiments include a comparison between the LNBR energy and a global region energy, similar to the data term of the Chan-Vese model. The implementation of the latter on the explicit polygon raises the difficulty of computing region integrals. A naive solution consists in using region filling algorithms to determine inner pixels [6] which would be computationally expensive if performed after each deformation step. Another solution, which we chose, is based on a discretization of Green-Riemann theorem. We compute and store the summed intensities P and Q in the respective directions x and y only once, before deformation is performed. This reduces the algorithmic complexity to $O(n)$, whereas the LNBR term induces a $O(nB)$ complexity.

3.2 Implicit representation

On the other hand, we provide an implicit implementation of the LNBR energy. In this case, the contour is the zero level set of $\psi : \mathbb{R}^2 \to \mathbb{R}$. We define the region

enclosed by the contour as $R_{\mathrm{I}} = \{\mathbf{x}|\psi(\mathbf{x}) \leq 0\}$. Function ψ evolves according to the following PDE:

$$\frac{\partial \psi}{\partial t} = F(\mathbf{x}) \left\|\nabla \psi(\mathbf{x})\right\| \ \ \forall \mathbf{x} \in \mathbb{R}^2$$

where speed function F is to some extent the level set-equivalent of the explicit energy in eq. (1), i.e. a weighted sum of smoothness and region terms:

$$F(\mathbf{x}) = \omega F_{\mathrm{smooth}}(\mathbf{x}) + (1-\omega) F_{\mathrm{LNBR}}(\mathbf{x})$$

where the smoothness term is expressed as usual using curvature. Areas and average intensities on the outer band are easily computed on the level set implementation, since a circular window of radius B may be considered around each pixel located on the front.

$$\mathcal{B}_{\mathrm{O}} = \{\mathbf{x}|\psi(\mathbf{x}) \geq 0 \text{ and } \exists \mathbf{y} \in \mathcal{W}_B(\mathbf{x}) \text{ s.t. } \psi(\mathbf{y}) = 0\}$$

Considering the sign of ψ, pixels belonging to $\mathcal{B}_{\mathrm{O}}$ are easily determined by dilating the front with circular window $\mathcal{W}_B$. As regards the average intensity along outward normal lines, we rely on the curvature-based formulation of the explicit curve. In the level set framework, it gives:

$$\mu_{\mathrm{LN}}(\mathbf{x}) = \frac{2}{B(2 + B\kappa_\psi(\mathbf{x}))} \int_0^B I(\mathbf{x} + b\mathbf{n}_\psi(\mathbf{x}))(1 + b\kappa_\psi(\mathbf{x}))db$$

with unit outward normal $\mathbf{n}_\psi$ and curvature κ_ψ:

$$\mathbf{n}_\psi(\mathbf{x}) = \frac{\nabla\psi(\mathbf{x})}{\|\nabla\psi(\mathbf{x})\|} \qquad \kappa_\psi(\mathbf{x}) = \mathrm{div}\left(\frac{\nabla\psi(\mathbf{x})}{\|\nabla\psi(\mathbf{x})\|}\right)$$

Computed as is, in order for $\mathbf{n}_\psi$ to be actually normal to the front, ψ should remain a distance function. This implies to update ψ as a signed Euclidean distance in the neighborhood of the front before estimating normal vectors. From eq. (7), we write the level set formulation of the LNBR term:

$$E_{\mathrm{LNBR}}[\psi] = \iint_{\mathcal{D}} (1 - H(\psi(\mathbf{x})))(I(\mathbf{x}) - \mu_{\mathrm{I}})^2 d\mathbf{x}$$
$$+ \iint_{\mathcal{D}} \delta(\psi(\mathbf{x})) \int_0^B (I(\mathbf{x} + b\mathbf{n}_\psi(\mathbf{x})) - \mu_{\mathrm{LN}}(\mathbf{x}))^2 (1 + b\kappa_\psi(\mathbf{x}))dbd\mathbf{x}$$

where H and δ are the Heaviside step and Dirac impulse functions. For a point $\mathbf{x}$ located on the front, the corresponding speed is approximated from eq. (10):

$$F_{\mathrm{LNBR}}(\mathbf{x}) = (I(\mathbf{x}) - \mu_{\mathrm{LN}}(\mathbf{x}))^2 - (I(\mathbf{x}) - \mu_{\mathrm{I}})^2$$

Eventually, the reader may note that an equivalent bias technique as the one used in the explicit implementation (see eq. (11)) is applied in the level set model. The level set function ψ evolves according to the narrow band technique [2], so that only pixels located on the front are updated.

4 Results and discussion

4.1 Concurrent methods

We compare the behavior of explicit and implicit active contours endowed with different data terms: an edge term [19], a global region term similar to one of the Chan-Vese model [7] and the uniform modeling energy of Lankton-Tannenbaum [12]. The goal of our experiments is not to compare explicit and implicit implementations, since it is well accepted that both exhibit their own advantages. We intend to show the interest of the LNBR energy whatever implementation is used. In the edge-based model, the region force is replaced by an edge force resulting from the differentiation of the image gradient magnitude:

$$\mathbf{f}_{\text{edge}}(\mathbf{p}_i) = \nabla \left\| \nabla G_\sigma * I(\mathbf{p}_i) \right\| - \alpha \mathbf{n}_i$$

where α weights an additional balloon force [18] increasing the capture range and consequently allowing the snake to be initialized far from the target boundaries. The gradient magnitude is computed on data convolved with first-order derivative of gaussian G_σ, where scale σ is empirically chosen to yield the most significant edges. A similar speed term F_{edge} is implemented in the level set contour. As stated by their authors, the Chan-Vese (CV) and Lankton-Tannenbaum (LT) models directly rely on an implicit formulation of the curve. We give their corresponding region speed terms:

$$F_{\text{global}}(\mathbf{x}) = (I(\mathbf{x}) - \mu_{\text{I}})^2 - (I(\mathbf{x}) - \mu_{\text{O}})^2$$

$$F_{\text{LT}}(\mathbf{x}) = \iint\limits_{\mathcal{W}_B(\mathbf{x})} \delta(\psi(\mathbf{y}))(I(\mathbf{y}) - \mu_{\text{I}}(\mathbf{x}))^2 - (I(\mathbf{y}) - \mu_{\text{O}}(\mathbf{x}))^2 d\mathbf{y}$$

where $\mu_{\text{I}}(\mathbf{x})$ is the local inner average intensity over the ball of radius B centered at $\mathbf{x}$, and similarly for the local outer average intensity $\mu_{\text{O}}(\mathbf{x})$. One may note that in the initial paper by Chan and Vese, the region term is asymmetric, as inner and outer terms are independently weighted, so that the variance minimization may be favoured inside or outside. However, we chose to use a symmetric term, as it is commonly the case with region-based active contours. Incidentally, future experiments could be done using asymmetry on all compared region terms. Moreover, the localized term of Lankton-Tannenbaum suffers from a weak capture range, since the front cannot evolve if inner and outer local means are similar. Thus, we also embedded into this energy the bias force of eq. (11). We used the same curvature-based regularization term for all tested approaches.

For all datasets, the model was initialized as a small circle fully or partially inside the area of interest, far from the target boundaries. Results are shown in fig. 3. Explicit contours are drawn in red whereas implicit ones appear in blue. For all experiments, the regularization weight ω was set to 0.5. On noisy data, we found that contours with lower ω were prone to boundary leaking. In addition,

insufficient regularization makes level set implementations leave spurious isolated pixels inside and outside the inner region. Conversely, values above 0.8 turn out to prevent the surface from propagating into narrow structures. Experiments are carried on grayscale and color images as well. For the latter ones, we should point out that the minimal variance principle is easily extended to vector quantities. Let us consider the vector-valued image $\mathbf{I}$ and average intensities $\mathbf{m}_{\mathrm{I}}$ and $\mathbf{m}_{\mathrm{LN}}$. In the inner term, the integrand becomes $\|\mathbf{I}-\mathbf{m}_{\mathrm{I}}\|^2$ and similarly for the outer term. The synthetic image in row 3, made up of color ellipses corrupted with gaussian noise, was segmented using RGB values. The natural images depicted in rows 4 to 7 hold nearly color-uniform objects. They were segmented using the ab components of the perceptually uniform CIE Lab color space. Neglecting the brightness L makes color statistics insensitive to illumination changes in visually uniform regions, allowing to handle highlights and shadows properly.

4.2 A note on the choice of the band thickness

The band thickness B is an important parameter of our method and should be discussed. Apart from its impact on the algorithmic complexity - computing average intensities along normal lines takes at least $O(nB)$ operations - it controls the trade-off between local and global features around the object. If $B = 1$, the region energy is as local as an edge term. The main image property having an effect on the minimal band thickness is the edges sharpness. Indeed, the deformable curve needs a larger band as the boundaries of the target object are fuzzy. To put this phenomenon into evidence, we applied the active contour on an increasingly blurred image. Bands thinner than the minimal one caused the contour to flow into neighboring structures. The original image was segmented with $B = 2$. For subsequent images, increasing the band turned out to be necessary. As the blur level of the last image in the sequence is rarely encountered in the applications we aim at, $B = 10$ was a suitable value in our experiments.

4.3 Segmentation results

Since we are looking for perceptually homogeneous objects, segmentation quality can be assessed visually. One can reasonably admit that the target object corresponds to the area containing the major part of the initial region. Gradient-based deformable models fail on images where noise and low contrast between neighboring objects prevent the extraction of reliable edges. Except for the last image in fig. 3, we could not find a suitable balloon weight preventing the contour from being trapped in spurious noisy edges inside the shape while stopping on the actual boundaries. Indeed, the edge-based energy is inefficient when the sharpness of boundaries decreases, as the contour may pass through the actual edges and stop on false ones simultaneously. In order to keep a critical eye on our approach, we draw the attention on the equivalence between the global and local region energies in particular images.

Row 2 and 4 depict typical configurations where there is no particular benefit in using localized region energies. In the MRI short-axis view of the human heart, the background is not uniform but still significantly darker than the bright left ventricle. Thus, the global region speed manages to make the front stabilize on the actual boundaries. The background of image 4 is obviously color-uniform as well. However, in other images containing various objects surrounding the structure of interest, the global region term captures all areas considered as different from the background. By definition, any two-phase segmentation model may fail at recovering a particular object when it is surrounded by many different objects, except in very particular cases such as a bright object surrounded by several dark objects. This phenomenon is well illustrated in row 3. Due to the averaging performed over the outer region, the global region approach turns out to split the image with respect to the blue component, since it is the dominant color in the background and it is absent of all areas in the inner region. Row 1 is a particular case in which the contour endowed with the global region-based active contour does not manage to grow, as inner and outer average intensities are not sufficiently different.

In the extent of our experiments, the Lankton-Tannenbaum method turns out to somewhat more sensitive to initialization than the LNBR active contour. In row 2, an inner dark papillary muscle is partially included in the initial region, which results in its incorporation into the final inner region. Since the Lankton-Tannenbaum energy only implies uniformity over balls centered at boundary pixels, it tends to flow into outer parts and leave some inner parts, as shown in rows 4, 5 and 6. The LNBR energy performs better at segmenting uniform objects. As a final remark, computational times imputed to the explicit contour fall between 0.5s and 1s on images of average size 512×512, with a C++ implementation running on an Intel Core 2 Duo 2GHz with 1Gb RAM. On the same images, we found the level-set implementations 3 to 4 times slower.

5 Conclusion

We have presented in this paper a local region-based method for deformable contours, relying on the assumption of a piecewise uniform background in the vicinity of the target object. The approach is based on a novel region term implying average intensities along lines in the outward direction normal to the curve. Based on the theory of parallel curves, a mathematical development was carried out in order to express the region energy in a form allowing natural implementation on explicit models. The local normal-based region energy managed to overcome the drawbacks of deformable models relying exclusively on edge terms or global region terms. We provided explicit and level-set based implementations. Very promising results were obtained in grayscale and color images. Further investigations will be performed in embedding local region terms into more geometrically constrained models. We also plan to extend the model to

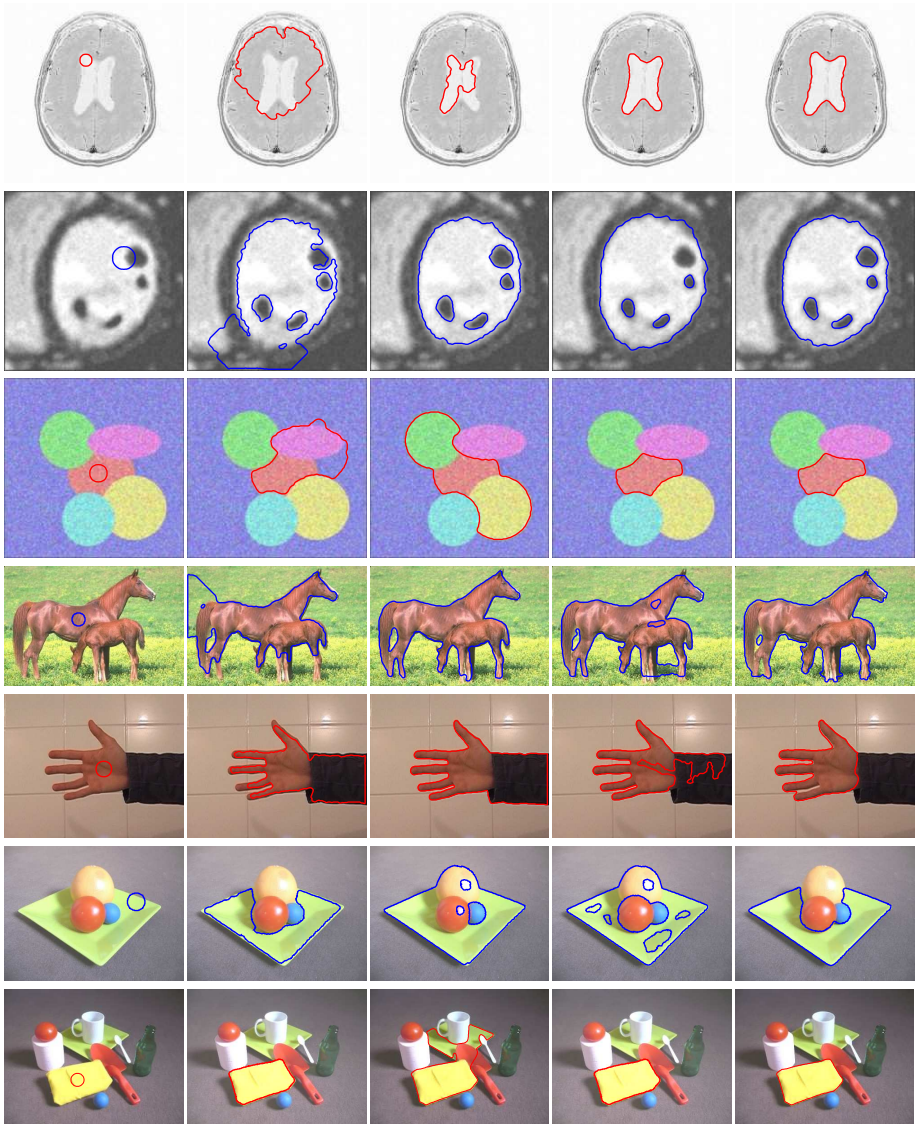

Fig. 3. Segmentation results on medical and natural color images. Starting from common initializations shown in column 1, the LNBR term is compared with three other energies (edge energy, global region energy and local uniform modeling energy of Lankton-Tannenbaum). The image in row 4 was taken from the Berkeley Segmentation Dataset [20]

temporal segmentation, in order to track evolving objects in videos, and to textured images.

A Calculus of variations

A.1 Derivative of parallel curve-based term

In classical active contours, curve Γ is a local minimizer of the functional

$$\mathcal{E}[\Gamma] = \int_{\Omega} \mathcal{L}(\mathbf{c}, \mathbf{c}_u, \mathbf{c}_{uu})\ du$$

when the following variational derivative vanishes:

$$\frac{\delta \mathcal{E}[\Gamma]}{\delta \Gamma} = \frac{\partial \mathcal{L}}{\partial \mathbf{c}} - \frac{d}{du}\left\{\frac{\partial \mathcal{L}}{\partial \mathbf{c}_u}\right\} + \frac{d^2}{du^2}\left\{\frac{\partial \mathcal{L}}{\partial \mathbf{c}_{uu}}\right\} \tag{12}$$

Considering now a functional expressed on the parallel curve,

$$\mathcal{E}'[\Gamma_{[B]}] = \int_{\Omega} \mathcal{L}'(\mathbf{c}_{[B]}, {\mathbf{c}_{[B]}}_u) du,$$

determining directly the derivative of $\mathcal{E}'[\Gamma_{[B]}]$ with respect to Γ leads to tedious calculations. Instead, we find more practical to determine $\delta\mathcal{E}'[\Gamma_{[B]}]/\delta\Gamma_{[B]}$ first, and then relate it to $\delta\mathcal{E}'[\Gamma_{[B]}]/\delta\Gamma$ using the following general expression:

$$\begin{aligned}\frac{\delta \mathcal{E}'}{\delta \Gamma} = {} & (1+B\kappa)\left\langle \frac{\delta \mathcal{E}'}{\delta \Gamma_{[B]}}, \mathbf{t} \right\rangle \mathbf{t} + (1-B\kappa)\left\langle \frac{\delta \mathcal{E}'}{\delta \Gamma_{[B]}}, \mathbf{n} \right\rangle \mathbf{n} \\ & + \frac{B\|\mathbf{c}_u\|_u}{\|\mathbf{c}_u\|^2}\left\langle \frac{\delta \mathcal{E}'}{\delta \Gamma_{[B]}}, \mathbf{t} \right\rangle \mathbf{n} - \frac{B}{\|\mathbf{c}_u\|}\left\langle \frac{d}{du}\left\{\frac{\delta \mathcal{E}'}{\delta \Gamma_{[B]}}\right\}, \mathbf{t} \right\rangle \mathbf{n}\end{aligned} \tag{13}$$

where $\langle , \rangle$ is the L^2 inner product and $\mathbf{t}$ is the unit tangent vector. To some extent, we designed the expression in eq. (13) as a chain rule for parallel curve-based energies. Hereafter, we use it to determine the derivative of the LNBR term.

A.2 Derivative of region terms

We now need to express derivatives of general region terms over R_{I} and $\mathcal{B}_{\mathrm{O}}$. Region terms are transformed into boundary integrals using Green's theorem. In this way, inners terms are differentiated according to the following template formula (the detailed derivation may be found for example in the appendix of [21]):

$$\frac{\delta}{\delta \Gamma}\left\{\iint_{R_{\mathrm{I}}} f(\mathbf{x}) d\mathbf{x}\right\} = -\|\mathbf{c}_u\|\, f(\mathbf{c})\mathbf{n} \tag{14}$$

Integrals over $\mathcal{B}_{\mathrm{O}}$ are more conveniently differentiated when expressed with integrals over R_{I} and its dilated counterpart $R_{\mathrm{I}[B]}$. Since $\mathcal{B}_{\mathrm{O}} = R_{\mathrm{I}[B]} \backslash R_{\mathrm{I}}$, we have:

$$\frac{\delta}{\delta \Gamma} \left\{ \iint\limits_{\mathcal{B}_{\mathrm{O}}} f(\mathbf{x}) d\mathbf{x} \right\} = \frac{\delta}{\delta \Gamma} \left\{ \iint\limits_{R_{\mathrm{I}[B]}} f(\mathbf{x}) d\mathbf{x} \right\} - \frac{\delta}{\delta \Gamma} \left\{ \iint\limits_{R_{\mathrm{I}}} f(\mathbf{x}) d\mathbf{x} \right\} \tag{15}$$

From eq. (14), we have:

$$\frac{\delta}{\delta \Gamma_{[B]}} \left\{ \iint\limits_{R_{\mathrm{I}[B]}} f(\mathbf{x}) d\mathbf{x} \right\} = - \left\| \mathbf{c}_u \right\| (1 + B\kappa) f(\mathbf{c}_{[B]}) \mathbf{n}$$

which is intuitively obtained by substituting Γ with $\Gamma_{[B]}$. In eq. (13), we replace $\delta \mathcal{E}_{[B]} / \delta \Gamma_{[B]}$ with the previous result. Since $\langle \mathbf{n}, \mathbf{t} \rangle = 0$, the derivative eventually reduces to:

$$\frac{\delta}{\delta \Gamma} \left\{ \iint\limits_{R_{\mathrm{I}[B]}} f(\mathbf{x}) d\mathbf{x} \right\} = - \left\| \mathbf{c}_u \right\| (1 + B\kappa) f(\mathbf{c}_{[B]}) \mathbf{n} \tag{16}$$

A.3 Derivative of LNBR energy

To determine the derivative of E_{LNBR}, we consider eqs (14), (15) and (16) and instantiate f with $(I - \mu_{\mathrm{I}})^2$ or $(I - \mu_{\mathrm{LN}})^2$ where appropriate. We approximate the derivative of the outer term of the LNBR energy from the derivative of the general integral $J(f, \mathcal{B}_{\mathrm{O}})$. Doing this, average intensities μ_{I} and μ_{LN} are assumed to be curve-independent. This is actually a shortcut since they do obviously depend on Γ (see eq. (6)). However, one may note that a similar derivation is made in the work by Chan-Vese [7], where average intensities μ_{I} and μ_{O} are initially formulated as variables and, by means of gradient descent, are actually assigned to average intensities. Finally, we have:

$$\frac{\delta E_{\mathrm{LNBR}}}{\delta \Gamma} \approx \left\| \mathbf{c}_u \right\| \left[-(I(\mathbf{c}) - \mu_{\mathrm{I}})^2 - (1 + B\kappa)(I(\mathbf{c}_{[B]}) - \mu_{\mathrm{LN}})^2 + (I(\mathbf{c}) - \mu_{\mathrm{LN}})^2 \right] \mathbf{n} \tag{17}$$

References

1. Kass, M., Witkin, A., Terzopoulos, D.: Snakes: active contour models. International Journal of Computer Vision **1**(4) (1988) 321–331
2. Malladi, R., Sethian, J., Vemuri, B.: Shape modeling with front propagation: a level set approach. IEEE Transactions on Pattern Analysis and Machine Intelligence **17**(2) (1995) 158–175
3. Brox, T., Cremers, D.: On the statistical interpretation of the piecewise smooth Mumford-Shah functional. In: International Conference on Scale Space and Variational Methods in Computer Vision (SSVM), Ischia, Italy (2007) 203–213

4. Mumford, D., Shah, J.: Optimal approximation by piecewise smooth functions and associated variational problems. Communications on Pure and Applied Mathematics **42**(5) (1989) 577–685
5. Cohen, L., Bardinet, E., Ayache, N.: Surface reconstruction using active contour models. In: SPIE Conference on Geometric Methods in Computer Vision, San Diego, CA, USA (1993)
6. Ivins, J., Porrill, J.: Active region models for segmenting textures and colours. Image and Vision Computing **13**(5) (1995) 431–438
7. Chan, T., Vese, L.: Active contours without edges. IEEE Transactions on Image Processing **10**(2) (2001) 266–277
8. Jehan-Besson, S., Barlaud, M., Aubert, G.: DREAM^{2}S: Deformable regions driven by an eulerian accurate minimization method for image and video segmentation. International Journal of Computer Vision **53**(1) (2003) 45–70
9. Paragios, N., Deriche, R.: Geodesic active regions and level set methods for supervised texture segmentation. International Journal of Computer Vision **46**(3) (2002) 223–247
10. Vese, L., Chan, T.: A multiphase level set framework for image segmentation using the Mumford and Shah model. International Journal of Computer Vision **50**(3) (2002) 271–293
11. Alemán-Flores, M., Alvarez, L., Caselles, V.: Texture-oriented anisotropic filtering and geodesic active contours in breast tumor ultrasound segmentation. Journal of Mathematical Imaging and Vision **28**(1) (2007) 81–97
12. Lankton, S., Tannenbaum, A.: Localizing region-based active contours. IEEE Transactions on Image Processing **17**(11) (2008) 2029–2039
13. Li, C., Kao, C., Gore, J., Ding, Z.: Implicit active contours driven by local binary fitting energy. In: IEEE Computer Vision and Pattern Recognition (CVPR), Minneapolis, Minnesota, USA (2007) 17–22
14. Piovano, J., Papadopoulo, T.: Local statistic based region segmentation with automatic scale selection. In: European Conference on Computer Vision (ECCV). Volume 5303 of LNCS., Marseille, France, Springer (2008) 486–499
15. Elber, G., In-Kwon, L., Myung-Soo, K.: Comparing offset curve approximation methods. IEEE Computer Graphics and Applications **17**(3) (1997) 62–71
16. Pressley, A.: Elementary differential geometry. Springer (2002)
17. Charpiat, G., Maurel, P., Pons, J.P., Keriven, R., Faugeras, O.: Generalized gradients: priors on minimization flows. International Journal of Computer Vision **73**(3) (2007) 325–344
18. Cohen, L.: On active contour models and balloons. Computer Vision, Graphics, and Image Processing: Image Understanding **53**(2) (1991) 211–218
19. Caselles, V., Kimmel, R., Sapiro, G.: Geodesic active contours. International Journal of Computer Vision **22**(1) (1997) 61–79
20. Martin, D., Fowlkes, C., Tal, D., Malik, J.: A database of human segmented natural images and its application to evaluating segmentation algorithms and measuring ecological statistics. In: IEEE International Conference on Computer Visison (ICCV). Volume 2., Vacouver, Canada (2001) 416–423
21. Zhu, S., Yuille, A.: Region competition: unifying snakes, region growing, Bayes/MDL for multiband image segmentation. IEEE Transactions on Pattern Analysis and Machine Intelligence **18**(9) (1996) 884–900